Local and Global Chain Dynamics in Diblock Copolymer Melts

G. Fytas, S. H. Anastasiadis, K. Karatasos and N. Hadjichristidis†

Foundation for Research and Technology – Hellas, P.O. Box 1527, 711 10 Heraklion, Crete, Greece

Abstract

Photon correlation spectroscopy in the depolarized mode and dielectric relaxation spectroscopy were employed to investigate local and global chain motions in poly(styrene-b-1,4-isoprene) diblock copolymer melts near the order-to-disorder transition (ODT). The presence of two distinctily different segmental orientation processes and the temperature dependence of the width of the slow relaxation function in the disordered state imply strong composition fluctuations in calorimetrically and rheologically homogeneous diblocks. The estimated amplitudes of composition fluctuations increase with the proximity to the ODT. The polyisoprene subchain orientation is characterized by a single broad distribution of relaxation times above the ODT, that apparently senses an average friction. This is due to the fact that the end-to-end vector orientations sample fluctuations at a different length scale than segmental orientations do.

1. Introduction

Diblock copolymers (A–B), consisting of a contiguous linear sequence of polymerized monomers of type A covalently bonded to a second contiguous linear sequence of chemically different monomers B, is an interesting class of polymeric materials with rich variety of phase behavior [1]. A significant feature of diblock copolymers is the order-to-disorder transition (ODT) with increasing temperature, T, and/or decreasing the overall degree of polymerizaton, N. The equilibrium phase morphology of a diblock copolymer melt can be controlled by a few experimental parameters as discussed in the next section. Hence the equilibrium composition field configurations and their coherence may probably be varied to investigate the manifestation of the composition heterogeneities on the local and overall chain motion in A–B melts.

In contrast to the static properties, there has been little theoretical and experimental work done on the rich segmental and global chain dynamics of either disordered or ordered A–B melts. The relaxation function $C(t)$ of the orientation fluctuations can be measured by photon correlation (PCS) [2] and/or dielectric relaxation (DS) [3] spectroscopy over a broad dynamic range $(10^{-6}–10^3\,\text{s})$ at temperatures near the glass transition temperature, T_g. The dielectrically observed $C(t)$ may be sensitive to both local (segmental) and long wavelength (normal mode) orientational motions of chains with finite dipole moment component parallel to the chain contour [4]. The relaxational characteristics, i.e., rate and time distribution functions of the two processes will, in principle, sense different effective composition fluctuations at two length scales.

Here, we report on PCS and DS experimental work on the segmental and chain relaxation in the composition field configurations of poly(styrene-b-1,4-isoprene) (SI) copolymers in the vicinity of ODT. The presence of two distinctly

different segmental orientation processes near and above ODT implies bimodal probability distribution of the composition in a macroscopic volume, whereas friction effects alone cannot account for the I-chain orientation.

2. Theoretical background

The ensemble of molecular configuration that produces the minimum overall free energy represents the equilibrium state in a block copolymer melt. Diblock copolymers are single component systems that cannot macrophase separate. However, unfavorable interaction between the A and B blocks, expressed by the segment–segment Flory–Huggins interaction parameter, χ, may lead under certain conditions to a local segregation of dissimilar monomers. The equilibrium phase morphology of diblock copolymers is determined by the overall degree of polymerization, N, the overall volume fraction of, e.g., the A block, f, and χ which depends on temperature as $\chi = \alpha + b/T$, with $b > 0$. Since the entropic and enthalpic contributions to the free energy density scale as N^{-1} and χ, respectively, it is the product χN that dictates the equilibrium phase morphology for a certain composition f [1]. For $\chi N \ll 1$, the equilibrium morphology is a melt with uniform composition (homogeneous or disordered state). As χN increases to be $O(10)$, a delicate balance between entropic and enthalpic factors leads to an order-disorder transition (ODT) towards a microphase characterized by long range order in its composition with characteristic size of the order of the size of the molecules [5] and a sinusoidal ordered composition profile.

In a seminal theoretical work, Leibler [5] constructed a Landau expansion of the free energy to fourth order in a compositional order parameter field, $\psi(r) = \phi_A(r) - f$, where $\phi_A(r)$ is the microscopic volume fraction of A monomers at position r, and he was able to map out the phase diagram of a diblock copolymer near the ODT in the parameter space χN vs. f; he predicted a critical point for $f_c = 0.5$ at $(\chi N)_c = 10.5$, where a symmetric diblock undergoes a second-order phase transition from the disordered to the lamellar phase. Fredrickson and co-workers [6] incorporated the fluctuation corrections in the effective Hamiltonian for a diblock melt in the Hartree approximation, and found that the fluctuation corrections, controlled by a Ginsburg parameter, $\bar{N}$, defined [6, 7] by $\bar{N} = 6^3(R_g^3\rho_c)^2$, where ρ_c is the number density of copolymer chains in the melt, lead to a suppression of the symmetric critical mean field point that is replaced by a weak first-order transition at a lower temperature [6], with the amplitude of the ordered composition profile predicted to be $O(\bar{N}^{-1/6})$ at the ODT. Besides the uniform field in the disordered phase and the perfectly ordered sinusoidal configuration of wavelength $2\pi/q^* \cong O(R_g)$ in the ordered phase [5], the Hartree approximation

---

† Also at University of Athens, Department of Chemistry, Athens, Greece.

also weights configurations that have superimposed isotropic composition plane waves with wave vectors having random orientations and phases and a preferred or not magnitude, q^*. The theory suggests that the root-mean-squared amplitude of these fluctuations is $O(\bar{N}^{-1/6})$, comparable to the amplitude of the long-range ordered composition field, with the typical equilibrium field configurations ("pattern") in the disordered diblock melt (which fluctuate in time) speculated [7] to be reminiscent of the transient non-equilibrium patterns encountered during the intermediate and late stages of spinodal decomposition. The structure factor $S(q)$ for a monodisperse diblock is modified from Leibler's mean field result by replacing χ with an effective interaction parameter, χ_{eff}, which depends on temperature, molecular weight, and composition and is related to the bare parameter. The Hartree structure factor near the ODT may be approximated by the Lorentzian form $S(q) = S_0/[1 + \xi^2(q - q^*)^2]$, where the susceptibility $S_0 = (\varepsilon \rho_c)^{-1}$, and the coherence length of composition fluctuations $\xi = \sqrt{6} c R_g [F(x^*, f) - 2\chi_{eff} N]^{-1/2}$, with c a composition-dependent constant [6]. The fluctuations amplitude at the transition is predicted as $a_1 = 1.0057[c^3(x^*)^3/C(f)]^{1/6} \bar{N}^{-1/6}$, where c, x^*, and $C(f)$ are constants depending on f [6].

The strong significance of composition fluctuations in the disordered state near the ODT has been recently reported, by small angle neutron scattering and rheological investigations on a series of near symmetric monodisperse diblocks [7], in qualitative and quantitative agreement with theory [6]. In this manuscript we will summarize the clear evidence, obtained by PCS and DS, of the existence of two distinctly different segmental orientation times in "homogeneous" diblock copolymer melts, which proves the existence of two different local environments in diblocks, i.e., strong compositon fluctuations even far above the ODT.

3. Segmental relaxation

The molecular characteristics of the four SI sample are listed in Table I [8–11]. All samples but SI-4 are in the disordered state and they display a single broad glass transition intermediate between the T_g's of the pure components. Based on this observation spatial homogeneity down to about 100 Å is conceivable implying a unimodal probability distribution $P(\varphi)$ of the composition fluctuations at these length scales. Compatiblity at shorter length scales can be assessed by probing local molecular processes. We employed PCS in the depolarized light scattering geometry [8] and DS [9] to selectively probe segmental dynamics in

styrene- (S-) and isoprene-rich (I-rich) microregions of the SI copolymer melts.

Two segmental modes are evident in the orientation correlation function $C_{VH}(t)$ measured in the depolarized scattering geometry of the PCS experiment. The fast relaxation process in the $C_{VH}(t)$ and its inverse Laplace transform of Fig. 1(a) compares favorably with the dielectric loss $\varepsilon''(\omega)$ and, hence, is assigned to local orientation dynamics in I-rich microenvironments of the SI-2 copolymer melt. The slow relaxation mode in $C_{VH}(t)$, and the distribution $L (\log \tau)$ associated with segmental motion within S-rich microregions, can hardly be resolved in the $\varepsilon''(\omega)$ spectrum due to the weak dipole moment of S segments. Since the temperature of Fig. 1(a) is lower than the single T_g of SI-2, the motion of S segments in S-rich microenvironments is frozen, as revealed by the insensitivity of the slow mode of the distribution of the orientation times, $L (\log \tau)$, to T variations below about 273 K [8].
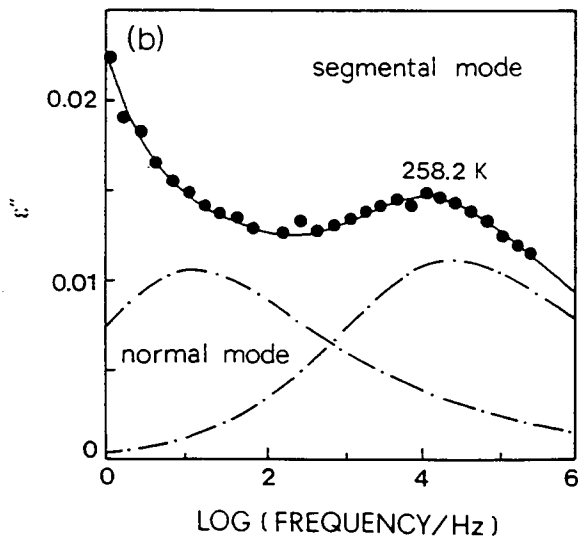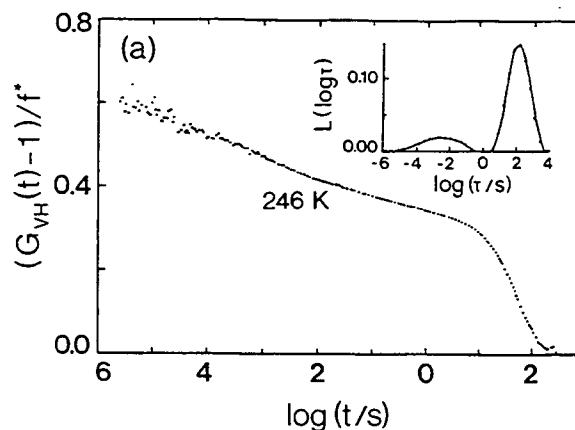
Table I. Molecular characteristics of the samples

Sample[†]	$M_n/10^3$	w_{PI}	f_{PI}	N	$(\chi N)_{25°C}$	T_g/K
SI-1[a]	4.4	0.36	0.39	51	4.8	284
SI-2[a]	5.7	0.50	0.54	68	6.1	255
SI-3[b]	7.8	0.38	0.41	95	8.4	276
SI-4[c]	9.9	0.41	0.42	121	10.8	228 and 325
SI-5[a]	3.9	0.28	0.31	48	4.5	308

† I: isoprene; S: styrene.
[a] References [8, 9].
[b] Reference [10].
[c] Reference [11].

Fig. 1. (a) Depolarized intensity correlation function $|C_{VH}(t)|^2$ for SI-2 and the corresponding distribution $L (\log \tau)$ of orientation times (inset) obtained from the inverse Laplace transformation of $C_{VH}(t)$ at 246 K [8]. (b) Dielectric loss ε'' vs. frequency for SI-2 at 258 K. The solid line indicates the superposition of two relaxation processes [9].

The two orientation times τ_s and τ_f obtained from the peak positions in L (log τ) and $\varepsilon''(\omega)$ of the PCS and DS experiments respectively are much more separated in time than those observed for athermal copolymers [12]. The situation is illustrated in the Arrhenius plot of the two segmental orientation times in three of the disordered SI copolymers of Table I. The segmental times in bulk PI and PS homopolymers are also shown in Fig. 2 for comparison. For PS homopolymer, two solid lines are drawn to account for the different T_g's of the S-subchain in SI-1, SI-2 ($T_g = 340\,K$) and SI-3 ($T_g = 352\,K$), whereas for the segmental motion in bulk PI a molecular weight independent T_g was used ($= 206\,K$).

Despite the calorimetrically and rheologically observed homogeneity of the three SI copolymers, the two distinct time scales of Fig. 2 imply significant demixing at shorter length scales. The conformational transitions responsible for segmental orientation, usually involve few monomer units [13]. The relevant correlation volume, V_α, is given by

$$V_\alpha = 2\pi \int_0^\infty F(r)r^2 \, dr \qquad (1)$$

with $F(r)$ being the orientation correlation function of segments located a distance r apart. Now, if the composition correlation length ξ (Section 2 above) exceeds $\xi_\alpha \propto (V_\alpha)^{1/3}$, then the presence of slow composition fluctuations ("pattern" relaxation [14]) would enhance the non-exponentiality of the segmental relaxation function and hence the breadth of L (log τ) in disordered copolymers. The dual character of the distribution L (log τ) implies a bimodal probability distribution $P(\varphi)$ in the subvolumes V_α. In fact, according to very recent computer simulation [15, 16] of diblock copolymer melts, $P(\varphi)$ can become bimodal near ODT if the sampling volume is sufficiently small. The large separation between τ_s and τ_f in the three SI copolymers implies significant disparity in the effective compositions, in for example isoprene, φ_I^S and φ_I^I of the two microregions rich in S and I respectively.

Estimates of these local average compositions at the poles of $P(\varphi)$ can be obtained from the two characteristic relaxation times within the concept of the free volume model [17,

18]. For a compatible mixture with volume fractions φ_A and φ_B, the activation parameter, B, and the ideal glass transition temperature, T_0, in the well-known VFT equation

$$\log \tau = \log \tau_0 + \frac{B}{T - T_0} \qquad (2)$$

with τ_0 being the limiting high temperature time, are given by mixing relations in terms of the values for the two components, i.e.:

$$\frac{1}{B} = \frac{\varphi_A}{B_A} + \frac{\varphi_B}{B_B}; \quad T_0 = \frac{\varphi_A T_{0A} B_B + \varphi_B T_{0B} B_A}{\varphi_A B_B + \varphi_B B_A} \qquad (3)$$

Assuming the same functions for the subvolume V_α, one can easily derive the expression for the local composition φ_A^K of component A in the K-rich microregions (A = S or I, and K = S or I) at a given T.

$$\varphi_A^K = \frac{B_A[B_B - \lambda_K(T - T_{0B})]}{\lambda_K[B_B(T - T_{0A}) - B_A(T - T_{0B})]} \qquad (4)$$

The parameters $\lambda_K \equiv \log \tau - \log \tau_0$ are computed from the experimental values of the segmental relaxation times in the K-rich microregion and setting $\tau_0 \cong 10^{-13}\,s$.

The effective local compositions in isoprene for the two microenvironments of the three SI samples are computed at $T \cong 290\,K$, for which both segmental processes can be probed. The computed values are not very different from those obtained from isochrone plots vs. temperature [14, 19, 20].

The bulk f_{PI} and the effective local compositions are shown in the mean field phase diagram of Fig. 3 which visualizes the proximity of the SI samples to the ODT. The amplitude of the composition fluctuations increases systematically with the proximity to the ODT, with the root-mean-squared amplitude ranging from 0.21 to 0.37, in agreement with the theoretical estimates [6]. We should note, however, that for all but the SI-2 diblocks, the enrichment appears skewed towards the low T_g microenvironment. This might be attributed to the fact that, for the same T, these environments are farther from their T_g's; this will lead to probing fluctuations over smaller lengths, since $V_\alpha \propto (T - T_0)^{-2}$ [21]. The asymmetric concentration fluctuations have been recently discussed in terms of conformer fractions instead of volume fractions [22].
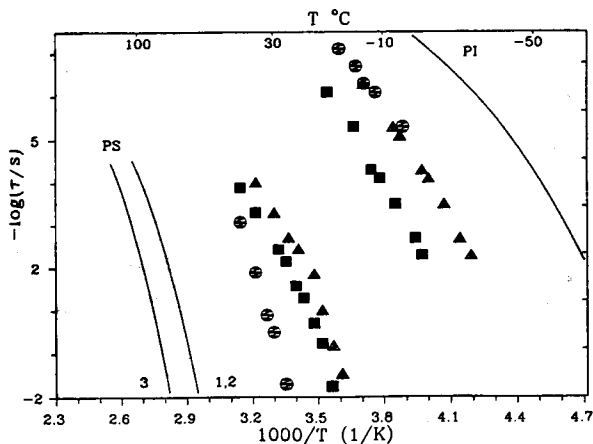

Fig. 2. Arrhenius plot of segmental orientation times for three homogeneous SI copolymers of Table I obtained by PCS and DS. ■, SI-1; ▲, SI-2; ●, SI-3. The solid lines represent the segmental orientation times in bulk PS and PI homopolymers of the same molecular weight (same T_g) of the respective blocks.
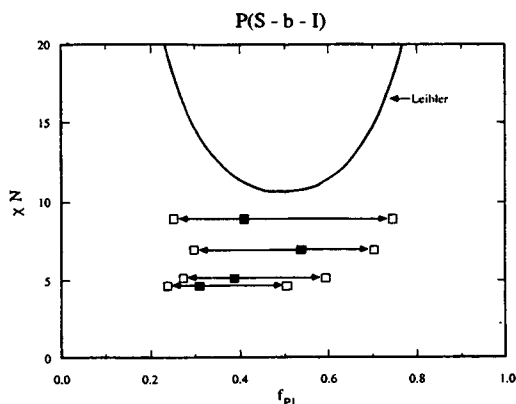

Fig. 3. Location of the homogeneous SI samples in the χN vs. f parameter space at about 290 K, relative to the mean-field [5] phase diagram. ■, average composition; □, effective local composition of the two microenvironments (see text).
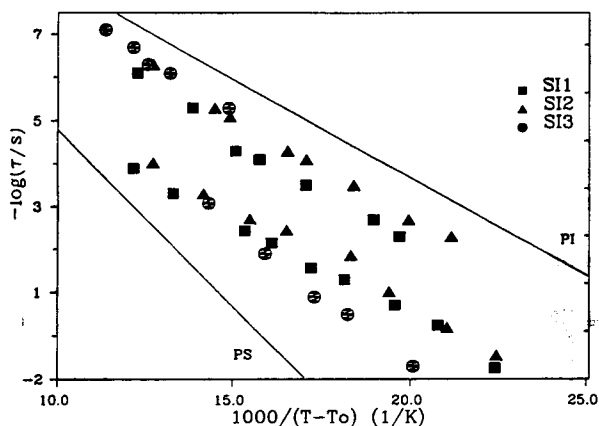
Fig. 4. A semilog reduced plot of the two segmental times in the SI copolymers vs. $T - T_0(\varphi^K)$. The ideal temperature T_0 [eq. (2)] is computed from eq. (3) at the local composition φ^K. ■, SI-I, ▲, SI-2; ●, SI-3. The solid lines represent the respective homopolymers.

The description of the segmental times τ_f and τ_s in terms of the free volume model [eqs (2)–(5)] led to physically meaningful local compositions and composition fluctuation amplitude. The large disparity in τ_f and τ_s values was attributed to the local segregation and, hence, two effective $T_0(\varphi^K)$ ($K = S$ or I environments) were invoked. In fact, a reduced plot can result from the representation of τ_f, τ_s vs. $1/[T - T_0(\varphi^K)]$ according to eq. 2. Such a plot is shown in Fig. 4, where it is found that the data from the S-rich environments behave similarly to the reduced homopolymer styrene, whereas the data from the I-rich microregion follow the behavior of isoprene homopolymer. The differences in the slope are due to differences in the $B(\varphi^K)$ parameters.

Composition fluctuations are also manifested in the distribution function L (log τ) causing an excess broadening beyond that of the bulk homopolymers. The distribution L (log τ) for the SI copolymers reveals both broadening and narrowing temperature effects discussed elsewhere [8, 20].

4. Chain end-to-end fluctuations

Polyisoprene is one of the few known polymers with non-vanishing dipole moment component parallel to the chain contour and, hence, large scale chain motions (normal mode) are dielectrically active [4]. These motions should, in principle, sense structural and dynamical heterogeneities in diblock copolymer melts through the effective segmental friction ζ, the chain dimension, and the interactions near the S–I junction points.

Figure 5 displays the experimental dielectric loss $\varepsilon''(\omega)$ as a function of T and frequency ($\omega = 2\pi f$) for SI-3 sample. The normal and segmental mode of I subchain are respectively the higher and lower peak. The normal mode relaxation of I block in disordered SI exhibits a broader shape compared with the equivalent PI homopolymer but is narrower than the segmental relaxation function [9]. The T-dependence of the τ_n, obtained from the frequency at which the $\varepsilon''(\omega)$ of the normal mode attains its maximum value, is shown in Fig. 6 for three SI copolymers, together with the τ_n for the equivalent molecular weight polyisoprene homopolymers.

The temperature dependence of τ_n is similar to the corresponding τ_n of PI homopolymer with equivalent chain
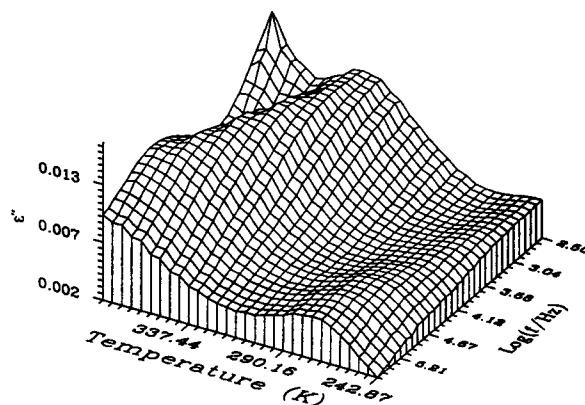
length, whereas the typical N^2-dependence predicted and found in unentangled PI homopolymers is obscured in the SI copolymer melts. A kink that has been observed in the T-dependence of τ_n [9, 18] may be a signature of the freezing of the S-segments [8, 9] rather than a manifestation of the ODT [18].

A self-consistent representation of the τ_n values of Fig. 6 in terms of eqs (2)–(4) and in analogy to the segmental times yields an effective φ for overall I-subchain motion indistinguishable from the bulk composition f. Actually, the calculated normal mode curve based on average friction is shown in the inset of Fig. 6, and it is indistinguishable from the experimental points. In this description, we have used the B_A, T_{0A} values of the segmental relaxation of PS homopolymer and the B_B, T_{0B} values of the normal mode relaxation of an equivalent PI homopolymer [23]. This result is not unexpected in view of the preceding section since the sampling subvolume ($V \propto R^3$, R: end-to-end distance) is now increased. Therefore, the probability distribution $P(\varphi)$ becomes unimodal for end-to-end chain fluctuations with width $\langle(\delta\varphi)^2\rangle_V$ smaller than $\langle(\delta\varphi)^2\rangle_{V_s}$. This is consistent
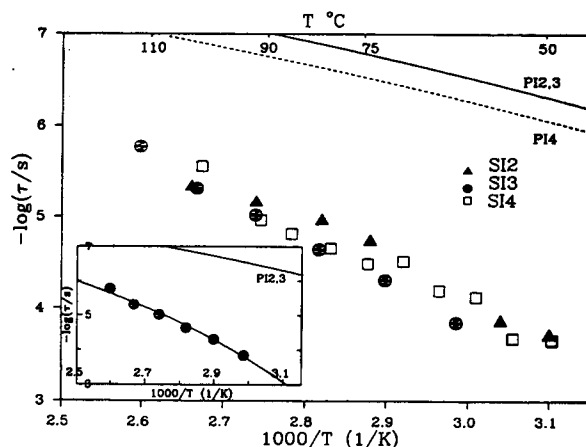

Fig. 5. Dielectric loss ε'' as a function of frequency and temperature for the disordered diblock SI-3. $\omega = 2\pi f$.

Fig. 6. Arrhenius plot of the relaxation time τ_n for the global chain orientation for three SI copolymers. ▲, SI-2; ●, SI-3, □, SI-4. The solid and dashed lines denote $\tau_n(T)$ for two PI homopolymer chains equivalent to SI-2,3 and SI-4, respectively. The comparison of experimental τ_n in SI-3 with a calculated τ_n based on the average friction of the disordered SI-3 is shown in the inset.

with the fact that the broadening of normal mode relaxation functions is less than for a segmental relaxation.

Very near and/or below the ODT, however, a splitting of the normal mode relaxation has been recently observed in bulk [11] and in solution in a common solvent [23]. Its origin is still under investigation, and is currently attributed to interfacial effects in the more or less permanent morphology formed below the ODT. This splitting should probably be related to the ODT.

5. Concluding remarks

In summary, we presented clear experimental evidence on the effect of the proximity to the ODT on local (segmental) and global chain (normal mode) relaxation in diblock copolymers. The presence of two distinctly different microenvironments in "homogeneous" diblocks is a manifestation of a bimodal probability distribution function, when sampled in the correlation volume V_α. The segmental relaxations may be accounted for in the free volume model by considering local compositions and composition fluctuation amplitudes. The normal mode relaxation, on the other hand, apparently senses a unimodal probability function due to the larger sampling volume, except very close and below the ODT.

Acknowledgements

References

1. Bates, F. S. and Fredrickson, G. H., Annu. Rev. Phys. Chem. 41, 525 (1990).
2. Fytas, G. and Meier, G., in: "Dynamic Light Scattering, the Method and Some Applications" (Edited by W. Brown) (Oxford University Press, London 1993), ch. 9, p. 407.
3. Boese, D., Momper, B., Meier, G., Kremer, F., Hagenah, J. U. and Fischer, E. W., Macromolecules 22, 4416 (1989).
4. Yao, M.-L., Watanabe, H., Adachi, K. and Kotaka, T., Macromolecules 24, 2955 (1991).
5. Leibler, L., Macromolecules 13, 1602 (1980).
6. Fredrickson, G. H. and Helfand, E., J. Chem. Phys. 87, 697 (1987); Barrat, J. L. and Fredrickson, G. H., J. Chem. Phys. 95, 1282 (1991).
7. Bates, F. S., Rosedale, J. H. and Fredrickson, G. H., J. Chem. Phys. 92, 6255 (1990).
8. Rizos, A. K., Fytas, G. and Roovers, J. E. L., J. Chem. Phys. 97, 6925 (1992).
9. Alig, I., Kremer, F., Fytas, G. and Roovers, J. E. L., Macromolecules 25, 5277 (1992).
10. Rizos, A. K. and Hadjichristidis, N., unpublished (1992).
11. Karatasos, K., Anastasiadis, S. H., Fytas, G., Pispas, S. and Hadjichristidis, N., in preparation (1993).
12. Kanetakis, J., Fytas, G., Kremer, F. and Pakula, T., Macromolecules 25, 3484 (1992).
13. Bahar, I., Erman, B. and Monnerie, L., Macromolecules 22, 2396 (1989), and references therein.
14. Anastasiadis, S. H., Fytas, G., Vogt, S. and Fischer, E. W., Phys. Rev. Lett. 70, 2415 (1993); Vogt, S., Jian, T., Anastasiadis, S. H., Fytas, G. and Fischer, E. W., Macromolecules 26, 3357 (1993); Anastasiadis, S. H., Fytas, G., Vogt, S, Gerharz, B. and Fischer, E. W., Europhys. Lett. 22, 619 (1993).
15. Gauger, A., Weyersberg, A. and Pakula, T., Makromol. Chem., Theory Simul. 2, 531 (1993); Weyersberg, A. and Vilgis, T. A., Phys. Rev. E. 48, 377 (1993).
16. Marx, D., Nielaba, P. and Binder, K., Phys. Rev. Lett. 67, 3124 (1991).
17. Fujita, H., Fortrschr. Hochpolym. Forsch. 3, 1 (1961).
18. Stühn, B. and Stickel, F., Macromolecules 25, 5306 (1992).
19. Quan, X., Johnson, G. E., Anderson, E. W., Bates, F. S., Macromolecules 22, 2451 (1989).
20. Fytas, G. and Anastasiadis, S. H., in: "Disorder Effects on Relaxation Processes" (Edited by R. Richert and A. Blumen) (Springer-Verlag, Berlin 1993), in press.
21. Donth, E., J. Non-Cryst. Solids 131–133, 204 (1991).
22. Quan, X., Johnson, G. E., Matsuoka, S. and Pirz, M., Polymer Prepr. 34(2), 580 (1993); Matsuoka, S. and Quan, X., Macromolecules 24, 2770 (1991).
22. Boesse, D. and Kremer, F., Macromolecules 23, 829 (1990).
23. Yao, M.-L., Watanabe, H., Adachi, K., Kotaka, T., Macromolecules 25, 1699 (1992).